

Optimizing diffusion-driven flow in a fissure

Renaud Heitz and Thomas Peacock

Department of Mechanical Engineering, Massachusetts Institute of Technology, Cambridge, Massachusetts 02139

Roman Stocker

Department of Civil and Environmental Engineering, Massachusetts Institute of Technology, Cambridge, Massachusetts 02139

(Received 21 April 2005; accepted 8 November 2005; published online 9 December 2005)

Diffusion-driven flow arises when a stably stratified fluid is bounded by an inclined wall. For a stratified fluid in an inclined fissure, in which fluid is confined to a gap between two inclined parallel walls, the flow field is determined by the gap width and the angle of inclination. When the gap width is much wider than the buoyancy layer thickness, the problem reduces to that of a semi-infinite fluid. As the gap width decreases, interaction between the boundary layer flows on the upper and lower walls increasingly influences the velocity profile, affecting transport within the fissure. We have obtained supporting experimental results that show these trends, demonstrating the existence of optimum conditions for dye transport. © 2005 American Institute of Physics.

[DOI: [10.1063/1.2142833](https://doi.org/10.1063/1.2142833)]

The study of diffusion-driven flow in a fissure was motivated by a desire to understand transport along cracks in rocks over geological time scales.¹ Subsequent theoretical investigations of a water-filled fracture subject to the Earth's geothermal gradient found an increase of up to three orders of magnitude in the dispersion coefficient of a passive contaminant over molecular diffusion alone.² Furthermore, the importance of diffusion-driven flow in the transport of chemicals in porous material, such as concrete, has been revealed by numerical studies.³ To date, there have only been two experimental studies. One provided quantitative agreement with theory for a fissure inclined at 45°,⁴ while the other, by two of the present authors, corresponded to the special case of a fissure of infinite width.⁵

In this paper, we concern ourselves with the dependence of diffusion-driven flow in a fissure on the angle of inclination and gap width, revealing optimum conditions for transport and providing supporting experimental results. The fissure, shown in Fig. 1, comprises two impermeable parallel walls. The no-flux boundary condition requires that isopycnals (lines of constant density) meet each wall at a right angle, and therefore depart from the horizontal. This generates along-the-wall convection in a thin buoyancy layer in which viscous and buoyancy forces balance. Convection is up-slope along the lower wall and down-slope along the upper wall.

By assuming a steady unidirectional velocity field, Phillips¹ obtained an analytical solution for the along-the-wall velocity u as a function of the wall-normal coordinate η ($\eta=0$ in the middle of the fissure, as shown in Fig. 1):

$$u(\eta) = \frac{\Gamma g \cos \alpha}{2\gamma^3 \mu} [-F(\gamma d/2) \sin \gamma \eta \cosh \gamma \eta + G(\gamma d/2) \cos \gamma \eta \sinh \gamma \eta], \quad (1)$$

where d is the fissure width, α the angle of inclination, g the

acceleration of gravity, μ the dynamic viscosity, ρ the density, $\Gamma = -(\partial \rho / \partial z) \sin \alpha$ the component of the density gradient along the fissure, z the vertical coordinate (positive upwards),

$$\gamma^{-1} = \left(\frac{g \Gamma \sin \alpha}{4 \mu \kappa} \right)^{-1/4} \quad (2)$$

is a characteristic length scale of the buoyancy layer thickness, κ the molecular diffusion coefficient, and the functions F and G are defined as

$$F(X) = \frac{\sin X \cosh X}{\sin X \cos X + \sinh X \cosh X}, \quad (3)$$

$$G(X) = \frac{\sinh X \cos X}{\sin X \cos X + \sinh X \cosh X}.$$

For a fissure whose width greatly exceeds the buoyancy layer thickness ($d \gg \gamma^{-1}$), there is no interaction between the flows along either wall of the fissure. The limiting case is a fissure of infinite width, equivalent to a single wall in a semi-infinite plane, whose solution is given by Phillips¹ and Wunsch⁶ and was investigated experimentally by Peacock *et al.*⁵ As the gap width becomes comparable to the buoyancy layer thickness ($d \sim \gamma^{-1}$), interaction occurs between flows induced at the upper and lower walls and the two buoyancy layers partially merge in the middle of the fissure (see Fig. 1).

The upward volume flux Q_{up} along the lower wall is equal and opposite to the downward flux Q_{down} along the upper wall,

$$Q_{up} = \int_{-d/2}^0 u d\eta = -Q_{down} = \int_0^{d/2} u d\eta, \quad (4)$$

resulting in zero net volume flux along the fissure. There is a net mass flux, however, due to the stratification, which can

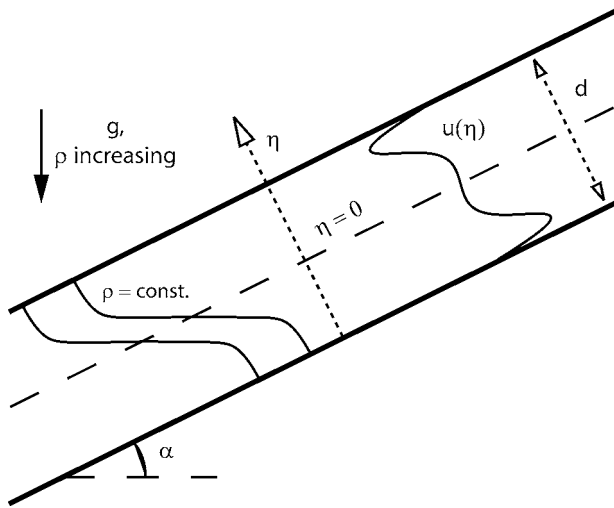


FIG. 1. Schematic of diffusion-driven flow in a fissure of width d inclined at an angle α to the horizontal. The isopycnals intersect the two walls at right angles to satisfy the no-flux boundary condition. The profile of the along-the-wall velocity u is shown as a function of the transverse coordinate η ($\eta=0$ at the centerline).

be significantly larger than that from diffusion alone.¹ The characteristic velocity at which material is transported by the flow in each half of the fissure is

$$\bar{u} = \frac{Q_{\text{up}}}{\min(d/2, \pi\gamma^{-1})}. \quad (5)$$

Here we take $\pi\gamma^{-1}$ as a working definition of the buoyancy layer thickness, corresponding to the distance from the wall of the first zero crossing of the semi-infinite velocity profile.⁷ This definition was previously and successfully used by Peacock *et al.*⁵ to determine the characteristic velocity of material transport by diffusion-driven flow in a semi-infinite fluid. Equation (5) accounts for the fact that in a fissure the buoyancy layer thickness cannot exceed $d/2$.

In Fig. 2 we plot \bar{u} for salt-stratified water ($\kappa = 10^{-9} \text{ m}^2 \text{ s}^{-1}$, $\mu = 10^{-3} \text{ kg m}^{-1} \text{ s}^{-1}$) as a function of d and α . In the limit of a fissure of infinite width, the velocity diverges as the angle tends to zero, and the unidirectional solution of Phillips¹ breaks down; this was verified experimentally by Peacock *et al.*⁵ For a fissure of finite width, γ^{-1} becomes comparable to d for sufficiently small α . The interaction between the velocity profiles along the two walls is then responsible for determining the angle α_{max} at which \bar{u} is maximized. Two significant features of (5) are highlighted by curves (a) and (b) in Fig. 2, showing the angular dependence of \bar{u} for $d=1.0$ and 1.5 mm, respectively: (i) \bar{u} goes to zero with α (unlike the semi-infinite case); (ii) α_{max} depends on the gap width. The second of these two features is emphasized by curve (c), which shows α_{max} as a function of d .

To verify the effects of inclination and gap width on diffusion-driven flow in a fissure, we carried out a series of experiments in an acrylic tank 40 cm long \times 25 cm high \times 2.5 cm wide, filled with salt-stratified water. A fissure, like that sketched in Fig. 1, was formed using two parallel pieces of acrylic. The acrylic pieces were 15 cm long, 2.3 cm wide, and 0.635 cm thick, and the fissure gap d (the spacing be-

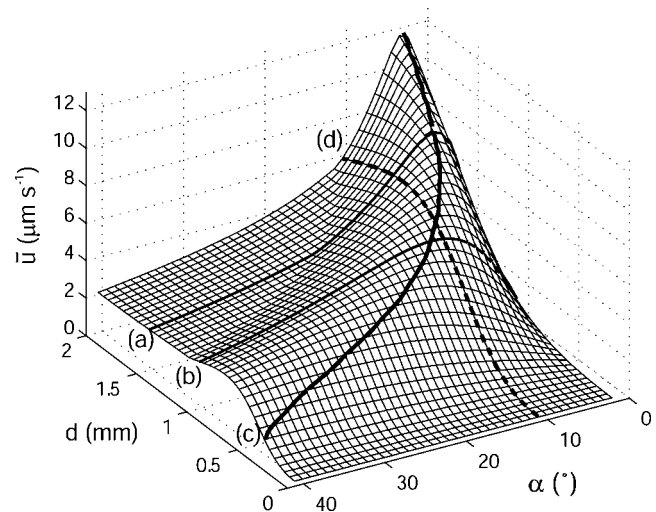


FIG. 2. Characteristic velocity \bar{u} [see Eq. (5)] along each wall of a fissure as a function of the gap width d and the angle of inclination α . The two curves labeled (a) and (b) correspond, respectively, to the gap widths 1 mm and 1.5 mm used in the experiments. The curve (c) highlights the maximum velocity for any given gap width. The curve (d) shows the mean velocity as a function of the gap width for $\alpha=10.5^\circ$.

tween the two pieces of acrylic) was set using a screw mechanism and measured to an accuracy of 0.05 mm using a Mitutoyo micrometer. The fissure was placed inside the acrylic tank, and there existed a 1 mm gap between either side of the fissure and the inside walls of the tank, to facilitate smooth filling of the tank. In principle, this small gap allowed flow into and out of the fissure along its edges, but in practice this was not found to be detrimental to the results. The angle of inclination α of the fissure with respect to the horizontal was set using support stands with a tolerance of 1.0° and measured to an accuracy of 0.1° from a digital image of the fissure and a plumbline. Once the fissure was positioned in the tank, a stratification was established by filling from below with salt water supplied by a double bucket system. The stratification was left to stabilize for one hour before the density gradient was measured in the body of the tank using a calibrated PME salinity probe. The density gradient across the depth of the tank was highly linear in all experiments, with a characteristic magnitude of 1050 kg m^{-4} ; given that the fissure was open to the tank at all sides, this was taken to be the stratification inside the fissure.

For visualization purposes, a small amount (~ 0.5 mL) of dyed neutrally buoyant fluid was slowly injected into a reservoir at the lower entrance of the fissure using a syringe pump. India ink was used to dye the fluid instead of the Blue Dextran employed in our previous study⁵, as the latter could not provide sufficient contrast for tracking flow in the narrow gap. The diffusion of the India ink was more noticeable than that of Blue Dextran (several mm over the course of an experiment), and this is accounted for in our estimates of the experimental error. Once emplaced, the dyed fluid from the reservoir was drawn into the fissure by diffusion-driven flow. To allow the flow to continuously adjust to the changing boundary conditions as it entered the fissure, the entrance

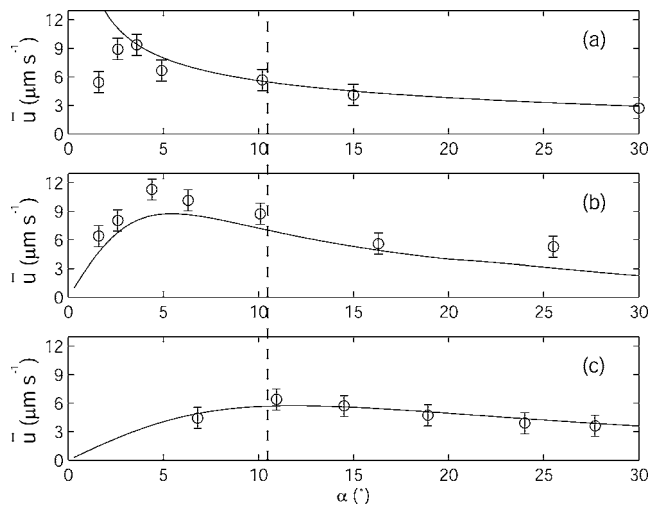


FIG. 3. Experimental results for velocity measurements of diffusion-driven flow in a fissure. (a) $d \rightarrow \infty$. (b) $d = 1.5$ mm. (c) $d = 1.0$ mm. The solid lines are the theoretical curves for \bar{u} , as defined in Eq. (5). The dashed line is $\alpha = 10.5^\circ$.

was machined so that the gap width varied smoothly from 8 mm to the desired fissure width d over an entrance length of 1 cm.

The advection of dye along the lower wall of the fissure was recorded using a digital camera with a resolution of 15 pixels/mm. Consistent with the theoretical flow field, depicted in Fig. 1, dye was transported upwards only in the lower half of the fissure, suggesting the existence of a return (downwards) flow in the upper half of the fissure. Images were taken at intervals of 2 min, and processed with MATLAB to locate the position of the dye front as a function of time. We used the same approach as Peacock *et al.*:⁵ the first image was subtracted from all subsequent ones, and the position of the dye front was defined as the furthest pixel along the fissure whose intensity satisfied a threshold requirement above the background noise level. The processed frames from this study were very similar to those in Peacock *et al.*,⁵ to which we refer the interested reader. Finally, the velocity was determined from a linear regression to the position of the dye front as a function of time.

The results are presented in Fig. 3, where we have plotted the measured velocity as a function of α for $d = 1.5$ and 1.0 mm. For comparison, Fig. 3 also presents the data from Peacock *et al.*⁵ for a semi-infinite fluid, corresponding to a fissure of infinite width. There is an additional data point at $\alpha = 10.2^\circ$ for the semi-infinite case and we note that this new point agrees very well with the previous results obtained using Blue Dextran. The solid line in each plot is the theoretical mean velocity \bar{u} , calculated using (5). We recall that the unidirectional theory breaks down at very small angles and large gap widths, hence the disagreement between experiment and theory at small angles in Fig. 3(a); this was the focus of the study by Peacock *et al.*⁵

Figure 3 shows good quantitative agreement between the

theoretical and measured velocities, highlighting several important features of diffusion-driven flow in a fissure. First, it is evident that the angle α_{\max} at which the mean velocity is maximized is indeed a function of the gap width. There is no theoretical result to compare with for $d \rightarrow \infty$, but the earlier experimental results of Peacock *et al.*⁵ presented in Fig. 3(a) imply a maximum near 2.8° . Performing a quadratic fit to the three points closest to the maxima in Figs. 3(b) and 3(c), we find for $d = 1.5$ mm that $\alpha_{\max} = 4.8^\circ$, and lies within the range 4.4 – 6.3° when experimental error is considered in the fitting. For $d = 1.0$ mm, the fitting gives $\alpha_{\max} = 11.6^\circ$, with a range 6.9 – 14.5° when experimental error is considered. These results agree well with their corresponding theoretical values: for $d = 1.5$ mm, $\alpha_{\max} = 5.4^\circ$ and for $d = 1.0$ mm, $\alpha_{\max} = 10.5^\circ$. The increase in α_{\max} is even more striking for smaller gap widths. For example, theory predicts $\alpha_{\max} = 33.3^\circ$ for $d = 0.5$ mm. We were unable to obtain data for gap widths significantly smaller than 1 mm, however, as the dye appeared to stall at the entrance to the fissure, and what little did enter, the camera had difficulty resolving.

The second feature highlighted by our results is that \bar{u} varies in a nontrivial manner with the gap width for a given angle of inclination. The dashed curve (d) in Fig. 2, showing the dependence of \bar{u} on d for $\alpha = 10.5^\circ$, exhibits a maximum at a gap width of 1.4 mm. Turning now to the experimental results, we have likewise drawn a dashed line through Figs. 3(a)–3(c) at $\alpha = 10.5^\circ$. Consistent with theory, the highest measured velocity was attained for $d = 1.5$ mm: for $d \rightarrow \infty$, $\bar{u} = 5.6 \mu\text{m s}^{-1}$; for $d = 1.5$ mm, $\bar{u} = 8.7 \mu\text{m s}^{-1}$; and for $d = 1.0$ mm, $\bar{u} = 6.4 \mu\text{m s}^{-1}$.

In conclusion, we have revealed that the transport of material by diffusion-driven flow in a fissure can be optimized using two parameters: the angle of inclination and the gap width. A detailed study of the theoretical solution previously obtained by Phillips¹ was supported by a carefully chosen set of experiments. The results can be applied to geophysical flows, and may also pave the way for more modern applications, such as miniature devices that rely on transport in small-scale channels.⁷

The authors acknowledge helpful contributions by Jeff Aristoff and Martha Buckley.

¹O. M. Phillips, "On flows induced by diffusion in a stably stratified fluid," *Deep-Sea Res.* **17**, 435 (1970).

²A. W. Woods and S. J. Linz, "Natural convection in a tilted fracture," *J. Fluid Mech.* **241**, 59 (1992).

³E. J. Shaughnessy and J. W. Van Gilder, "Low Rayleigh number conjugate convection in straight inclined fractures in rock," *Numer. Heat Transfer, Part A* **28**, 389 (1995).

⁴E. Luna, A. Córdova, A. Medina, and F. J. Higuera, "Convection in a finite tilted fracture in a rock," *Phys. Lett. A* **300**, 449 (2002).

⁵T. Peacock, R. Stocker, and J. Aristoff, "An experimental investigation of the angular dependence of diffusion driven flow," *Phys. Fluids* **16**, 3503 (2004).

⁶C. Wunsch, "On oceanic boundary mixing," *Deep-Sea Res.* **17**, 293 (1970).

⁷There is a typo in Eq. (4) in Peacock *et al.* (Ref. 5) that is missing the factor $1/\pi$.